Journal of King Saud University – Computer and Information Sciences 34 (2022) 6217–6228

Contents lists available at ScienceDirect

Journal of King Saud University – Computer and Information Sciences

journal homepage: www.sciencedirect.com

MultiNet: A deep neural network approach for detecting breast cancer through multi-scale feature fusion

Saikat Islam Khan [a], Ashef Shahrior [a], Razaul Karim [a,*], Mahmodul Hasan [a], Anichur Rahman [b]

[a] Dept. of Computer Science and Engineering, Mawlana Bhashani Science and Technology University, Tangail, Bangladesh
[b] Dept. of Computer Science and Engineering, National Institute of Textile Engineering and Research, Savar, Dhaka, Bangladesh

ARTICLE INFO

Article history:
Received 25 March 2021
Revised 12 July 2021
Accepted 2 August 2021
Available online 17 August 2021

Keyword:
Breast cancer
CAD
DenseNet-201
NasNetMobile
VGG16
Feature fusion

ABSTRACT

Breast cancer diagnosis from biopsy tissue images conducted manually by pathologists is costly, time-consuming, and disagreements among specialists. Nowadays, the advancement of the Computer-Aided Diagnosis (CAD) system allows pathologists to identify breast cancer more reliably and quickly.For this reason, interest in CAD-based deep learning models has been increased significantly. In this study, we propose a "MultiNet" framework based on the transfer learning concept to classify different breast cancer types using two publicly available datasets that include 7909 and 400 microscopic breast images, respectively. The proposed "MultiNet" framework is designed to provide fast and accurate diagnostics for breast cancer with binary classification (benign and malignant) and multi-class classification (benign, in situ, invasive, and normal). In the proposed framework, features from microscopy images are extracted using three well-known pre-trained models, including DenseNet-201, NasNetMobile, and VGG16. The extracted features are then fed into the concatenate layer, making a robust hybrid model. The proposed framework yields an overall classification accuracy of 99% in classifying two classes. It also achieves 98% classification accuracy in classifying four classes. Such promising results will provide the opportunity to use "MultiNet" framework as a diagnostic model in clinics and health care.

1. Introduction

Breast cancer is the most pre-eminent causal factor for cancer-related death for women in the age group of 20 to 59 years around the world (Bray et al., 2018). Malignant (cancer) cells gather in groups inside the tissues to form an abnormality called a lump then these cells spread across the body entering into the blood vessels. These cancer cells, through migration across the body, damage other tissues and organs. In recent studies it's been found that 29% of all newly diagnosed cancer cases among women are expected to be breast cancer (Siegel et al., 2012). Even men are also at risk of developing breast cancer. According to an estimation made in 2020, around 2,620 men will be diagnosed with breast cancer in the U.S., and approximately 520 cases may be fatal (Breast cancer facts, 2021). The survival rate from breast cancer is expected to increase to 80% if diagnosed in early stages (W.H. Organization et al., 2014). Mammography and biopsy are two common diagnosing methods used for breast cancer detection where radiologists and pathologists examine breast images and infected tissue samples for detecting early symptoms of breast cancer through tumor identification and classification (Chetlen et al., 2016; Bhargava and Madabhushi, 2016). Histopathology, the study of the tissue structure, is a cumbersome process and requires very experienced pathologists to examine tissue samples manually using a microscope for determining diseases. Pathologists perform binary classification of lesion: benign and malignant through biopsy. Through histology the complex and challenging identification of distinction between normal, benign and malignant lesion becomes possible and thus enables prognostic evaluation (López et al., 2012; Pöllänen et al., 2014).

Segmentation and classification tasks are performed through color and texture-based features of histopathological images (Szczypiński et al., 2014). Variable interpretations are perceived among different pathologists in histopathological images analysis

* Corresponding author.
E-mail addresses: bappy.10.cse.mbstu@gmail.com (S.I. Khan), ashahrior.cse.mbstu@gmail.com (A. Shahrior), razaulce15004@gmail.com (R. Karim), mahmodul.mbstu@gmail.com (M. Hasan), anis_cse@niter.edu.bd (A. Rahman).
Peer review under responsibility of King Saud University.

Production and hosting by Elsevier

https://doi.org/10.1016/j.jksuci.2021.08.004
1319-1578/

(Robbins et al., 1995) generating contradicting results. Difficulties in the manual assessment of WSI have laid the foundation for computer-assisted diagnostic (CAD) methods (Komura and Ishikawa, 2018). Algorithms for histopathological images are rapidly evolving in medical image analysis, but to obtain effective and highly accurate results, it is still crucial to have an automated method (Irshad et al., 2013; Veta et al., 2014; McCann et al., 2014).

Traditional and classical machine learning models are being used in various problem domains. Different life saving researches have been performed that includes medical brain mri images processing to identify alzheimer's disease (Karim et al., 2021) and the measurement of water quality (Khan et al., 2021). But, in classical machine learning methods for analyzing digital histopathological images, the dynamic nature of tasks like preprocessing, segmentation, extraction of features etc. deteriorates the system's performance and accuracy. The deep learning framework has been introduced to tackle the issues of conventional machine learning techniques by automatically executing the task of extraction in a fully end-to-end fashion and learn the input images' holistic features from low to high level for the process of classification (LeCun et al., 2015). Deep learning methods have recently gained notable achievements in a variety of domains such as Image Analysis (Collaboration, 2018), Signal Processing (Yildirim et al., 2019), Speech Recognition (Aytar et al., 2016), Face Recognition (Liu et al., 2015), brain MRI (Pereira et al., 2016), and CT Image Diagnosis of Lung and Liver Disease (Gao et al., 2018). Applications in histopathology imaging based on deep transfer learning have delivered high performance in several tasks (Talo, 2019). In this work, we present an automated breast cancer classification system using a "MultiNet" framework. This framework is used for classifying both binary (benign and malignant) and multiclass (benign, insitu, invasive, and normal) breast microscopy images. We use three CNN pre-trained models, including DenseNet-201, NasNet-Mobile, and VGG16, for extracting the features from the microscopy images. Afterwards, we have combined all of the features using a concatenation layer. The fusion features are then fine-tuned using two dense layers, two batch normalization layers, and two dropout layers, where the final dense layer with softmax activation function is used for the classification task. The key benefits of this work are summarized as follows:

- The "MultiNet" framework provides segmentation-free feature extraction techniques that do not require any handcrafted feature extraction approaches relative to the conventional machine learning methods.
- The proposed framework achieves significant performance on the benign images and does not misclassify any malignant images.
- The "MultiNet" framework performance is evaluated on both large and small datasets. Results indicate that our framework is competent for achieving high performance in both cases.

Organization: The remainder of the paper has been formed as follows: in Section 2, we discussed the literature review. Afterwards, the proposed "MultiNet" framework has been explained in detail, along with data pre-processing and data augmentation strategies in Section 3. The experimental setup and findings are presented thoroughly in Section 4. In Section 5, the comparative outcome analysis with future direction is shown. Finally, the conclusion is reached in Section 6.

2. Related works

Substantial amount of papers have been published concerning the autonomous detection and classification of histopathological images to detect numerous categories of breast cancer. Many of these works propose image processing and machine learning techniques exploring numerous features such as hue, patterns, or morphological textures. The performance of different approaches widely varies from the models adopted and the planned training strategies. In this section, a summarized discussion of such works is discussed in brief.

Nadia et al. proposed a deep learning technique for detecting Invasive Ductal Carcinoma (IDC), the most common subtype of breast cancer, in breast histological images and the classification of lymphoma subtypes. In both cases, they applied Residual CNN and compared it with the UNet and ResNet architectures. They suggested a SEF method based on Residual CNN and a softmax classifier to address the two cases that avoid hand-crafted pathological features and finally obtained an accuracy of 97.06% (Brancati et al., 2019). In another related work, Yusuf et al. suggested an automated detection of IDC method using deep transfer learner strategies with two CNN pre-trained models including ResNet-50 and DenseNet-161 on 277,524 image patches from the public histopathology dataset (Celik et al., 2020). Here DenseNet-161 and ResNet-50 achieved an accuracy level of 91.57% and 90.96% respectively, with only the last layers of the models utilized for training. In another work on novel CNN architecture by Ibrahem et al., the proposed model comprises 15 convolution layers and two fully connected layers with the comparative analysis of six different activation functions (Kandel and Castelli, 2020). The used dataset PatchCamelyon contained 220,000 annotated images for training and 57,000 unannotated images for testing. The developed model obtained the highest AUC of 95.46% in this study. Besides Araujo et al. classified hematoxylin and eosin-stained breast biopsy images into four classes, such as normal tissue, benign tissue, in situ carcinoma, invasive carcinoma, and another binary classification of carcinoma and non-carcinoma using extracted features with CNN and Support Vector Machine classifier (Arauo et al., 2017). Their achieved accuracies were 77.8% for four class and 83.3% for binary classification. Talo et al., in his proposed methodology, applied two CNN pre-trained models, including ResNet-50 and DenseNet-161 on both grayscale and color histopathology images (Talo, 2019). The DenseNet-161 performed well on grayscale images with an accuracy of 97.89%. On the other hand, ResNet-50 showed the best result with color images with the highest classification accuracy of 98.87%. Furthermore, Khan et al. approached deep learning framework utilizing the concept of transfer learning (Khan et al., 2019). Here features extracted from breast cytology images using CNN pre-trained architectures such as as- GoogLeNet, VGGNet, and ResNet were combined using the transfer learning approach. The integrated architecture yielded better results than each of the architectures individually with an accuracy of 97.52%. They also applied different data augmentation techniques to increase the data set size and solve the overfitting issue. In Motlagh et al. (2018), several ResNet model performances are compared where ResNet-V1-152 model gained the optimal outcome with an overall accuracy of 99.6% with 3000 epochs. Wang et al. in Wang et al. (2018) classified four types of breast cancer in histopathology images with the application of deep learning methods with hierarchical loss and global pooling. Here they had worked with a dataset of 400 test images where VGG-16 and VGG-19 models were applied as deep learning structures and had achieved 92% of average accuracy. Dimitropoulos et al. proposed a method where they automated the classification process through encoding histopathological images as VLAD on the Grassmann manifold. Their gained experimental classification rates are 95.8% and 91.38% respectively with their own dataset and BreakHis dataset (Dimitropoulos et al., 2017). Karthiga et al. in their work upon performing segmentation with k-means clustering applied DWT (Discrete Wavelet Transform) to perform classification with

the extracted subbands. Their implemented method on the BreakHis dataset produced accuracy of 93.3% in linear SVM, 92.7% in Quadratic SVM and 91.3% in Fine Gaussian SVM (Karthiga and Narasimhan, 2018). Nahid et al. proposed a novel DNN technique with Convolutional Neural Network (CNN), Long-Short-Term-Memory (LSTM), and a combination of CNN and LSTM for breast cancer image classification with the BreakHis dataset. The extracted features were utilized for decision making with Softmax and Support Vector Machine (SVM). The best results gained through this experiment are as follows – accuracy 91% on 200 dataset, precision 96% on 40 dataset (Nahid et al., 2018). Alzubaidi et al. in their work employed transfer learning to address and optimize both the challenges of training data lackings and classification hematoxylin-eosin-stained breast biopsy images into four classes: invasive carcinoma, in situ carcinoma, benign tumor and normal tissue on the test set of the microscopy ICIAR-2018 dataset with image-wise classification accuracy of 96.1% (Alzubaidi et al., 2020). Roy et al. proposed a patch-based classifier (PBC) using CNN with two different modes: OPOD and APOD. They had used ICIAR 2018 breast histology image dataset which comprises 4 different classes- normal, benign, in situ and invasive carcinoma. Their overall achieved accuracy is 87% on the hidden dataset of ICIAR-2018 (Roy et al., 2019). Yao et al. in their proposed deep learning model used two different types of neural networks – a CNN (DenseNet) and an RNN (LSTM) to classify hematoxylin-eosin-stained breast biopsy images into four classes (normal tissues, benign lesions, in situ carcinomas, and invasive carcinomas). The model was tested with three different types of datasets-BACH2018, Bioimaging2015, and Extended Bioimaging2015. This experiment yielded an accuracy of 97.25% (Yao et al., 2019).

3. Proposed methodology

This section illustrates how microscopic breast images classify by integrating different multi-scale transfer learning models. Fig. 1 demonstrates the proposed "MultiNet" framework used in this classification. This framework starts with extracting images and loading the labels from the dataset. Before splitting the dataset, several preprocessing techniques are performed. After that, an extensive data augmentation technique carries out to increase the dataset size. Finally, we train the model individually on BreakHis and ICIAR datasets, respectively, and evaluate the proposed "MultiNet" framework using the testing images. The details of the blocks related to the proposed framework are given in the following subsections.

3.1. Dataset

In this work, we use two publicly available datasets for evaluating the proposed "MultiNet" framework in breast cancer detection. The first one obtains from the Breast Cancer Histopathological Database (BreakHis), which is available online (Breast cancer histopathological database, 2021). This dataset comprises 7909 microscopic breast tumor images, where 2480 images are benign, and the other 5429 images are malignant. The benign microscopic images consist of 4 benign tumors, including adenosis, fibroadenoma, phyllodes, and tubular adenoma tumors. The malignant tumors used in this dataset are carcinoma, lobular carcinoma, mucinous carcinoma, and papillary carcinoma. The microscopic images were obtained from 82 patients with different magnifying factors, including 40X, 100X, 200X, and 400X. All the microscopy images were selected patient-wise rather than image-wise so that images from the same patients will not be distributed in both training and test set. Such distribution will help avoid information leakage issues and make the prediction more valid. The second dataset is the ICIAR 2018 Grand Challenge dataset, which is also available online (Iciar, 2018). This dataset is composed of 400 H&E stained breast histology microscopic images. The ICIAR dataset is divided into four major groups, including normal, insitu carcinoma, benign, and invasive carcinoma, where each group contains 100 breast microscopic images. Fig. 2 presents the sample of the images extracted from both datasets. Table 1 presents the additional details of the BreakHis and ICAIAR datasets, respectively.

3.2. Data-preprocessing stage

Several preprocessing steps have been employed before feeding the images into the fine-tuned multiscale transfer learning model (see Fig. 3). All the microscopic images in the BreakHis dataset are in.png format with three channel RGB where each channel is in 8-bit depth. The images have 700 × 460 pixels, which we have reduced by 224 × 224 pixels as per the transfer learning concept. We convert all the images into a Numpy array so that the model

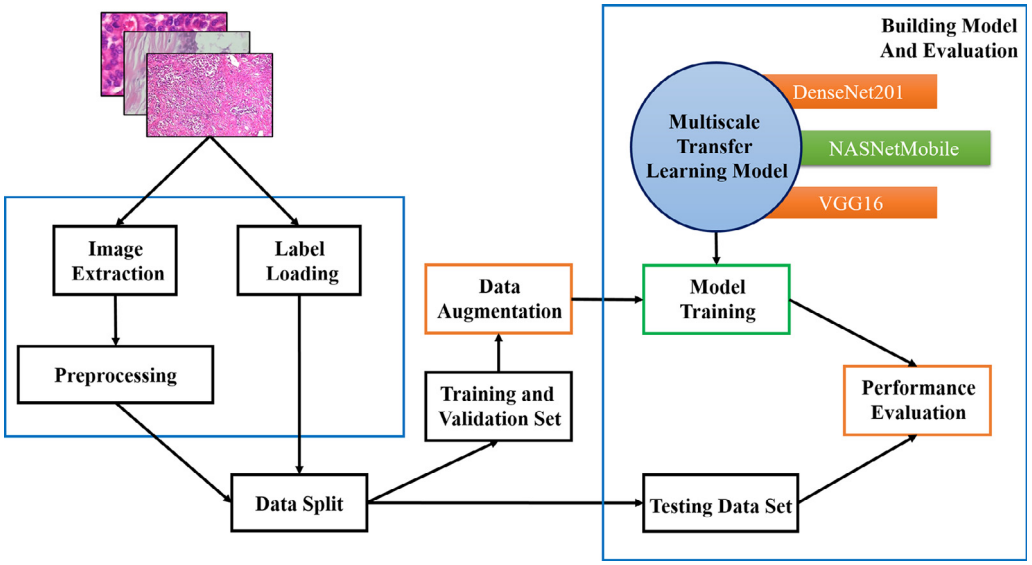

Fig. 1. Proposed "MultiNet" framework for the classification of microscopic breast images.

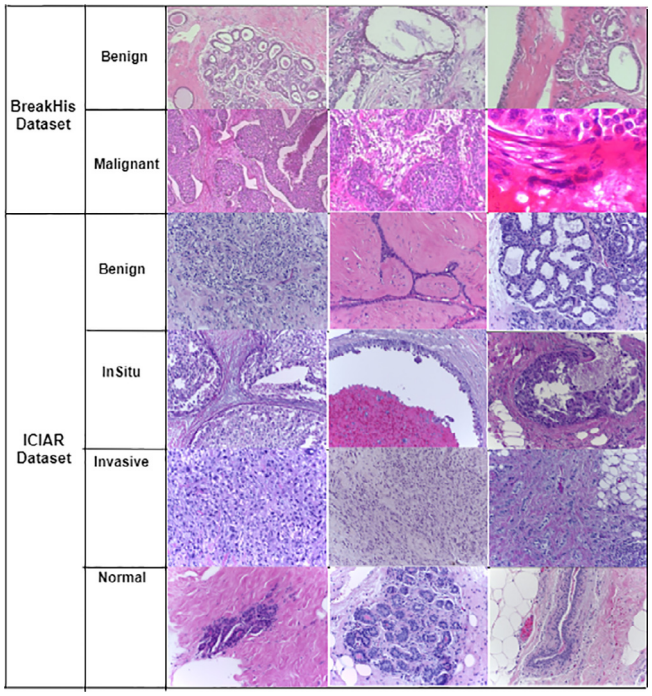

Fig. 2. Sample images from BreakHis and ICIAR dataset.

can train faster and takes less space into the memory. After that, we have shuffled the images so that the model can train on some unordered data. This dataset is divided into three steps, including training, testing, and validation, respectively. In this work, 70% of the data used for training, and the further 30% of the data used for validation and testing purposes. Several data augmentation techniques perform for different reasons, including increasing the dataset size, solving the overfitting issue, and making the model more robust (Wong et al., 2016). This dataset is increased from 7909 to 54403 after carrying out the data augmentation strategy. Further details of the data augmentation strategy are available in Table 3. On the other hand, all the microscopic images in the ICIAR dataset are in.tiff format, which we have converted to.jpeg format. We downsize the images' dimensionality from 1536 × 2048 pixels to 224 × 224 pixels as per the transfer learning concept. After that, we have followed the same approach as working with the BreakHis dataset. The number of images in the ICIAR dataset increased from 400 to 2560 after performing the data augmentation strategy. Table 2 presents the additional details of the datasets after data performing augmentation technique.

3.3. Building multi-scale transfer learning model

The multi-scale transfer learning model has been built by combining three well-known CNN pre-trained models, including DenseNet-201, NASNetMobile, and VGG16, respectively. Those models extract the low-level features separately from the breast microscopic images and then combined them using a fully connected layer for the classification task, as shown in Fig. 3. The integrated features represent high-level functionality such as sharpening, blur, textures, and gradient orientation of the microscopic images (Khan et al., 2021). After combining all the features, the proposed "MultiNet" framework has 37,767,702 parameters that are 3, 9, and 3 times more than the individual DenseNet-201, NASNetMobile, and VGG16 architectures, respectively. The basic structure of each adopted CNN pre-trained model and the fine-tuning process describes in the following sub-sections.

3.3.1. Dense convolutional networks (DenseNet)

The DenseNet pre-trained model was first developed by Huang et al. (2017), which had the best classification accuracy on CIFAR-10, CIFAR-100, and ImageNet dataset in 2017. This model developed similar to the ResNet architecture where each layer is feed forwarded to the other layers. Such connection gives the network to share important information within the model, which will make the network training more effective and boost the network performance (Hao and Zhang, 2019). In this work, we utilize the DenseNet-201 pre-trained model as our first feature extractor. This model consists of a total 201 deep CNN layers where each layer is arranged in such a way so that it can solve overfitting issues while dealing with a small dataset. Besides, the DenseNet-201 model provides significant enhancements to the ImageNet database by solving the gradient descent problem (Lumini and Nanni, 2019). Compared to the AlexNet, GoogLeNet, and ResNet architectures, the DenseNet-201 pre-trained model will derive more complicated and essential features as more deep CNN layers are included in this architecture.

3.3.2. NasNetMobile

The Google machine learning group first developed the NasNet-Mobile pre-trained model by training it on more than a million images on the Imagenet dataset (Zoph et al., 2018). This model obtained a 2.4% error rate in the CIFAR-10 dataset by introducing a new regularization technique called ScheduledDropPath. The NasNetMobile trains on 224 × 224 pixels input images where approximately 5.3 million training parameters are used. It is an optimized network consisting of fundamental building cells optimized by reinforcement learning. Such a cell consists of different convolution, pooling, and separable- convolution operations, making the model more reliable (Saxen et al., 2019).

3.3.3. Visual geometry group network (VGGNet)

The VGGNet pre-trained model was first developed by Simonyan and Zisserman et al., which obtained the first position for image localization and the second position for image classification at the ILSVRC competition 2014 (Simonyan and Zisserman, 2014). The VGGNet architecture showed an excellent performance compared to the AlexNet architecture by achieving an 8.1% error rate. In this work, we use VGG16 as our feature extractor. The VGG16 pre-trained model consists of 13 convolution layers, followed by three fully connected layers. All the convolution layers have a 3 × 3

Table 1
Additional information about two datasets before data augmentation.

Dataset	Breast Cancer Type	Training	Validation	Testing
BreakHis	Benign	1924	481	75
	Malignant	4274	1070	85
ICIAR	Normal	70	20	10
	InSitu Carcinoma	70	20	10
	Benign	70	20	10
	Invasive Carcinoma	70	20	10

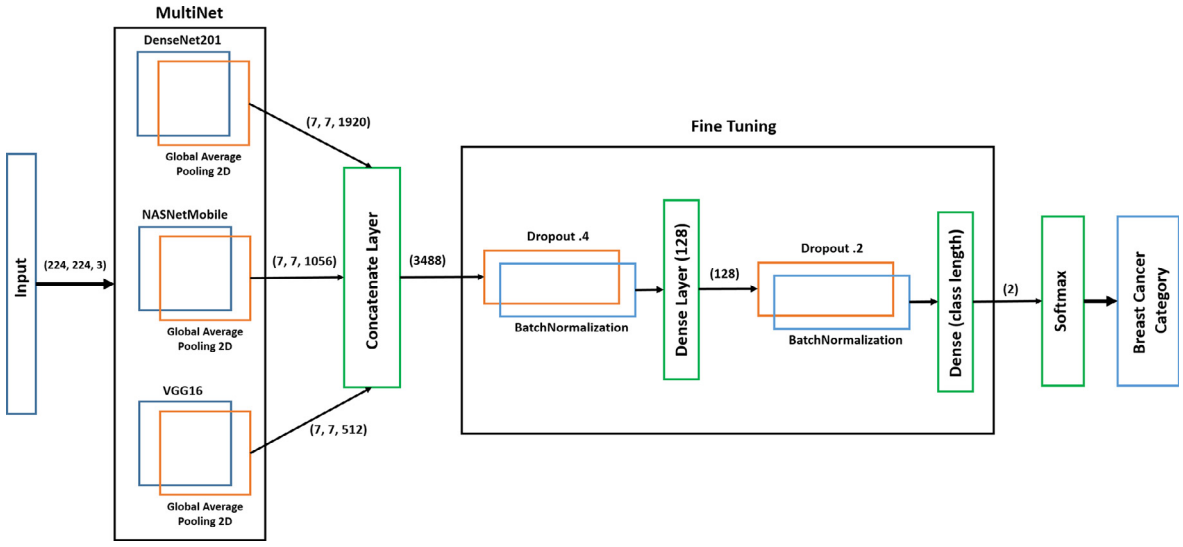

Fig. 3. Fine-tuned "MultiNet" framework.

Table 2
Additional information about two datasets after data augmentation.

Dataset	Breast Cancer Type	Training	Validation	Testing
BreakHis	Benign	13468	3367	75
	Malignant	29918	7490	85
ICIAR	Normal	490	140	10
	InSitu Carcinoma	490	140	10
	Benign	490	140	10
	Invasive Carcinoma	490	140	10

Table 3
Data augmentation strategies with parameter value.

Number	Data augmentation technique	Parameter value
1	Zooming range	2
2	Rotation range	90
3	Shearing range	.5
4	Width shift range	.4
5	Height shift range	.4
6	Horizontal flip	True
7	Vertical flip	True

windows size with a filter size ranging from 64 to 512. The pre-trained VGG16 architecture is divided into five blocks, where the first four convolution layers residing in the first two blocks and the other nine convolution layers residing in the next three blocks. A max-pooling layer also follows each block. The max-pooling layers have a 2×2 window size, which will extract the most dominant features from the transformed feature map (Scherer et al., 2010). In all convolution layers, the ReLU activation function is used.

3.4. Fine-tuning process

Fig. 3 presents how multiple transfer learning models integrate for classifying breast cancer categories using different fully connected layers. After extracting the features individually, all the pre-trained models use GlobalAveragePooling2D simultaneously for flattening all the layers into a vector by calculating the average value for each of the input channels. All the individual vectors are then combined into a single vector using the concatenate layer. After that, for fine-tuning the integrated features for our classification task, a total of six layers are used, followed by a softmax activation function. Following is the description of each layer.

Overfitting is a big issue in the deep neural network, which occurs when the model over-trained on the training data and negatively impacts the test data (Srivastava et al., 2014). To solve the overfitting issue, we use two dropout layers. The first dropout layer will exclude 40% of the data, and the second dropout layer will exclude 20% of the data during training the model. Besides, such an operation immensely helps in speeding up the training process (Srivastava et al., 2014).

Furthermore, we use two batch normalization layers, which plays a vital role in our classification model. The batch normalization layer will re-scale all the data so that we can normalize. The re-scaled data will help to accelerate the training phase and alleviate the sensitivity to network initialization. A dense layer is a fully connected layer where all the neurons in the previous and present layers are densely connected. Such layers operate on the input data and return an output. In our work, we use two dense layers where the last dense layer is used for the classification task, followed by a softmax activation function. This layer will take the length of the predicted class and make a prediction. The softmax activation function takes the probability of the outcome and determines which features are mostly correlated to the particular predicted class. The outcome value is between 0 and 1 in the softmax activation function, causing the neuron to trigger. It is defined as the following expression:

$$\text{softmax}(z)_j = \frac{\exp(z_j)}{\sum_{k=1}^{l} \exp(x_k)} \quad (1)$$

Table 4 presents the outcome of the integration between different transfer learning models and the fully connected layers. This table is extracted while building the "MultiNet" framework

Table 4
Details of "MultiNet" architecture.

Layer (type)	Output Shape	Param #	Connected to
input_1 (InputLayer)	(None, 224, 224, 3)	0	
densenet201 (Functional)	(None, 7, 7, 1920)	18321984	input_1 [0][0]
NASNet (Functional)	(None, 7, 7, 1056)	4269716	input_1 [0][0]
VGG16 (Functional)	(None, 7, 7, 512)	14714688	input_1 [0][0]
global_average_pooling2d (Global)	(None, 1920)	0	densenet201 [0][0]
global_average_pooling2d_1 (Global)	(None, 1056)	0	NASNet [0][0]
global_average_pooling2d_2 (Global)	(None, 512)	0	VGG16 [0][0]
concatenate_4 (Concatenate)	(None, 3488)	0	global_average_pooling2d [0][0] global_average_pooling2d_1 [0][0] global_average_pooling2d_2 [0][0]
dropout (Dropout)	(None, 3488)	0	concatenate_4 [0][0]
batch_normalization (Batch Normalization)	(None, 3488)	13952	dropout [0][0]
dense (Dense)	(None, 128)	446592	batch_normalization [0][0]
dropout_1 (Dropout)	(None, 128)	0	dense [0][0]
batch_normalization_1 (BatchNormalization)	(None, 128)	512	dropout_1 [0][0]
dense_1 (Dense)	(None, 2)	258	batch_normalization_1 [0][0]
Total Params: 37, 767, 702 Trainable Params: 37, 494, 676 Non-trainable Params: 273, 026			

for binary classification. That's why the last fully connected layer has two neurons. However, during working with multiclass classification, we use four neurons for the last dense layer. The other structure of the proposed "MultiNet" framework is same as working with the binary classification.

Algorithm 1 Automated breast cancer detection and classification.

1: **Input:** Breast cancer Training set $\delta 1$, Validation set $\delta 2$, and Testing set $\delta 3$.
$\alpha \leftarrow$ Learning rate.
$\beta \leftarrow$ Epochs.
$\mu \leftarrow$ Batch size.
$\gamma \leftarrow$ The number of images covered in one batch size.
Output: $\omega \leftarrow$ CNN pre-trained models weight.
begin: 2: Convert each microscopy image in training set into 224×224.
3: Perform data augmentation strategy for increasing the dataset size.
4: Extract the features from the microscopy images using DenseNet-201, NasNetMobile, and VGG16 CNN pre-trained models.
5: Combine the extracted features using the concatenate layer.
6: Set the fine-tuned layers CNN_{dense}, $CNN_{bathchnormalization}$, $CNN_{dropout}$, $CNN_{softmax}$.
7: Initialize the CNN pre-trained model parameters: α, β, μ, γ.
8: Train the "MultiNet" framework and determine the initial weights.
9: **for**$\beta = 1$ to β **do**
10: Select a mini batch size (size: γ) for training set $\delta 1$.
11: Forward propagation and determine the loss function.
12: Backpropagation and update the weight ω.
13: **end for**

4. Experimental setup, performance metrics and results analysis

This section demonstrates the experimental setup, hyperparameters used in the experiment, and the results obtained using the "MultiNet" framework from BreakHis and ICIAR datasets. A comparative analysis between the proposed method and the individual CNN pre-trained architecture is also discussed in depth.

4.1. Experimental setup

The proposed "MultiNet" framework was implemented using Keras, an open-source library that interfaced python with the neural network. We perform all the training and testing of the model using Google Colab, a free online cloud service that allows using Tesla K80 GPU with 12 GB of GDDR5 RAM, Intel Xeon processors with two cores @2.2 GHz, and a total of 13 GB ram.

4.2. Performance metrics

Different statistical parameters, including Precision, Recall, False-positive rate (FPR), and True negative rate (TNR), F1-Score, Matthews correlation coefficient (MCC), and Kappa Statistic are used to evaluate the proposed framework's performance. Such parameters depend on the outcome of the confusion matrix, including True Positive (TP), True Negative (TN), False Positive (FP), and False Negative (FN).

TP: refers to an outcome where the proposed "MultiNet" framework correctly identified the positive breast cancer type.

TN: refers to an outcome where the proposed framework correctly identified the negative breast cancer type.

FP: refers to an outcome where the proposed framework incorrectly identified the positive breast cancer type.

FN: refers to an outcome where the proposed framework incorrectly identified the negative breast cancer type.

All the statistical parameters are expressed as follows:

$$\text{Precision} = \frac{TP}{TP + FP} \tag{2}$$

$$\text{Recall} = \frac{TP}{TP + FN} \tag{3}$$

$$\text{FPR} = \frac{FP}{FP + TN} \tag{4}$$

$$\text{TNR} = \frac{TN}{TN + FP} \tag{5}$$

$$F1 - \text{score} = 2 \times \frac{\text{Pr} \times \text{Re}}{\text{Pr} + \text{Re}} \tag{6}$$

$$Kappa = \frac{Total\ Accuracy - Random\ Accuracy}{1 - Random\ Accuracy} \tag{7}$$

$$\text{MCC} = \frac{TP \times TN - FP \times FN}{\sqrt{(TP + FP)(TP + FN)(TN + FP)(TN + FN)}} \quad (8)$$

4.3. Training and parameter optimization

For the BreakHis dataset, Fig. 4 reflects the simulation result during training the proposed "MultiNet" framework. The hyper-parameter values used for training the framework presented in Table 5. One of the key hyper parameters to train a model is the optimizer function and the gradient descent's loss function. We choose adam as an optimizer function since it combines the key properties of the AdaGrad and RMSProp optimizers that can handle sparse gradient on a large dataset. We choose binary cross-entropy as a loss function since our work is based on binary classification in the BreakHis dataset. To decrease the loss function, we need an optimal learning rate value. However, choosing a learning rate is challenging since it produces undesirable behavior if the learning rate is quite large. If the learning rate is small, the model takes more time for training and makes tiny updates to the weights. In this work, we choose a learning rate of 0.0001, which will limit such issues. Furthermore, a small batch size of 32 has been used, which shows a suitable generalization of the model. The proposed framework trained for 50th epochs. However, after training only 29th epoch, the model managed to achieve more than 97 percent training accuracy and 98 percent validation accuracy. From Fig. 4 (a), we can also observe that the over-fitting issue is not present during training the model. While in the loss function curve Fig. 4 (b), it is clear that the curve starts to drop the loss value sharply. However, there are some fluctuations appeared due to the limited batch size of 32 images.

For the ICIAR dataset, Fig. 5 presents the accuracy progress and loss during training the proposed "MultiNet" framework. The hyper-parameter values used for training the framework are shown in Table 5. We choose categorical cross-entropy as a loss function since our work is based on the multiclass classification in the ICIAR dataset. In this dataset, the proposed model needed to be trained further due to the limited number of images. The "MultiNet" framework trained for 200th epochs, and right after the 166th epoch, 95 percent training accuracy has been achieved. Hence, the overall validation accuracy is reached during the validation phase is 94.4 percent. While in the loss function curve Fig. 5 (b), it is clear that the loss value is almost zero, and no fluctuations appeared during training and validating the model. From Fig. 5(a), it is also clear that the overfitting issue is not present.

Table 5
Parameter value used in the "MultiNet" framework during training.

Dataset	Parameter	Value
BreakHis	Optimizer	adam
	Learning Rate	.0001
	Loss Function	binary_crossentropy
	Metrics	accuracy
	Batch Size	32
	Epochs	50
ICIAR	Optimizer	adam
	Learning Rate	.0001
	Loss Function	categorical_crossentropy
	Metrics	accuracy
	Batch Size	32
	Epochs	200

4.4. Result analysis

The confusion matrix and the receiver operating characteristics (ROC) curve for the BreakHis dataset using the "MultiNet" framework are given in Fig. 6. The proposed framework combined three well-known transfer learning models, including DenseNet-201, NasNetMobile, and VGG16, and then use the fusion features for classifying whether the breast tissue is benign or malignant. It can be observed from Fig. 6(a) that a total of 74 and 85 microscopic images are correctly classified for benign and malignant breast cancer, respectively. At the same time, only one benign microscopic image is misclassified by the proposed framework. The most important benefit is that the "MultiNet" framework misclassifies no malignant breast cancer images in the BreakHis dataset. This framework also achieves an area value of 0.993 (see Fig. 6(b)), which indicates the consistency and stability of the model. Furthermore, all the transfer learning models are also individually performed on the BreakHis dataset to better understand the "MultiNet" framework's efficiency. Table 6 represents a comparative study between the "MultiNet" framework and the additional seven transfer learning models. It is clear from Table 6 that the "MultiNet" framework achieves an average precision of 0.99, recall of 0.99, f1-score of 0.99, kappa of.99, and MCC of.99, which outperforms all the other state-of-the-art mod-

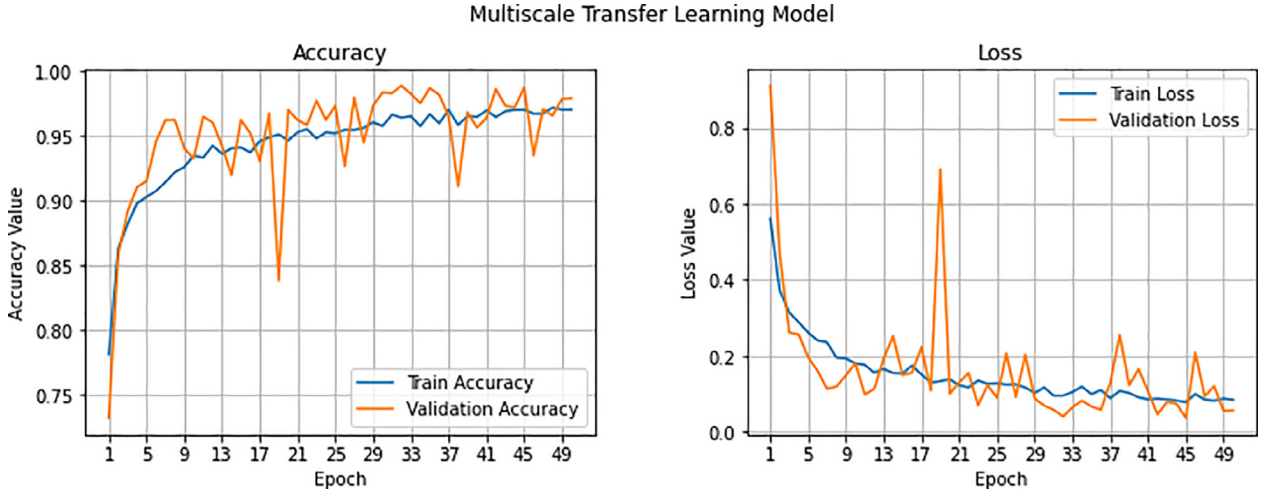

Fig. 4. Training progress for BreakHis dataset: (a) training and validation accuracy (higher is better), and (b) training and validation loss (lower is better).

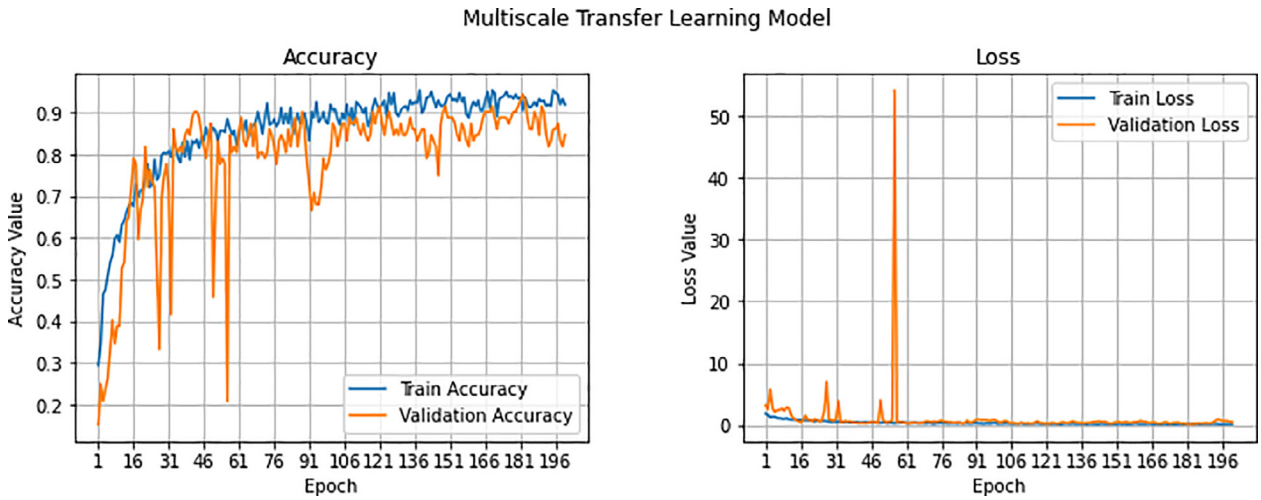

Fig. 5. Training progress for ICIAR dataset: (a) training and validation accuracy (higher is better), and (b) training and validation loss (lower is better).

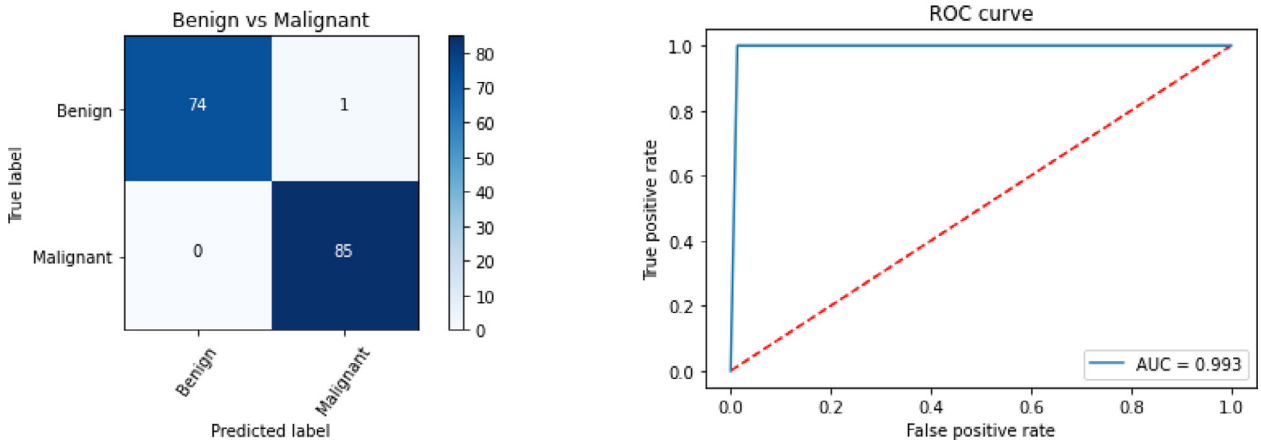

Fig. 6. "MultiNet" performance on BeakHis dataset a) confusion matrix b) ROC curve.

els. The FNR is almost 0, and the TNR is close to 1, indicating the model efficiency. However, the DenseNet-201 and Xception models also performed well by showing an average f1-score of 0.95 and.97. The other three models, including VGG16, VGG19, and NasNetMobile, have almost similar performance in detecting binary breast cancer category.

The confusion matrix and the ROC curve for the ICIAR dataset using the "MultiNet" framework are given in Fig. 7. In this dataset, the proposed framework identifies the multiclass breast cancer category, including benign, insitu, invasive, and normal. It can be observed from Fig. 7(a) that a total of 9, 10, 10, and 10 microscopic images are correctly classified for benign, insitu, invasive, and normal breast cancer category respectively. However, only one benign microscopic image is misclassified by the "MultiNet" framework. This framework achieves an area value of 0.956 (see Fig. 7(b)), indicating the model consistency and generality. A comparative analysis is also presented in Table 7, where it shows that the "MultiNet" framework achieves an average precision of 0.98, recall of 0.98, f1-score of 0.98, kappa of.97, and MCC of.97. It is also clear from Table 7 that the proposed framework has achieved high performance in detecting breast cancer categories compare to the other seven state-of-the-art models. Among the seven transfer learning models, the DenseNet-201, ResNet50, and Xception pre-trained models only manage to achieve more than 80% classification accuracy. However, the other four models perform poorly in detecting the multiclass breast cancer category.

5. Discussion

This paper proposes an approach for binary and multiclass breast cancer classification by applying a "MultiNet" framework to the microscopy images. We use two individual datasets for evaluating the "MultiNet" framework. The "MultiNet" framework's performance compared with the existing literature that has used the same dataset with different structures, parameters, and depths size are summarized in Table 8. It is clear from Table 8 that the proposed framework demonstrates the best prediction accuracy in the identification of both binary and multiclass breast cancer compared to the previous literature. We have obtained an average 99% and 98% classification accuracy for the BeakHis and ICIAR datasets, respectively, by correctly integrating all the pre-trained models. Fig. 8 presents some of the microscopy images that are predicted by the presented framework. However, there are some other advantages over the existing methods found in the literature. For example, some previous studies utilized different feature extractor methods, which is time-consuming and may

Table 6
Results obtained using the "MultiNet" architecture and seven individual transfer learning models on BreakHis Dataset.

Metrics	Model	Breast Cancer Category	TP	TN	FP	FN	Precision	Recall	FPR	TNR	F1-Score	Kappa	MCC
BreakHis Dataset	DenseNet-201	Benign	72	81	4	3	.95	.96	.05	.95	.95	.91	.91
		Malignant	81	72	3	4	.96	.95	.04	.96	.96	.91	.91
		Average Score					.95	.95	.04	.96	.95	.91	.91
	NasNetMobile	Benign	66	83	2	9	.97	.88	.02	.98	.92	.86	.86
		Malignant	83	66	9	2	.90	.98	.12	.88	.94	.86	.86
		Average Score					.93	.93	.07	.93	.93	.86	.86
	VGG-16	Benign	71	77	8	4	.90	.95	.09	.91	.92	.85	.85
		Malignant	77	71	4	8	.95	.91	.05	.95	.93	.85	.85
		Average Score					.92	.93	.07	.93	.93	.85	.85
	VGG-19	Benign	69	81	4	6	.95	.92	.04	.96	.93	.87	.87
		Malignant	81	69	6	4	.93	.95	.08	.92	.94	.87	.87
		Average Score					.94	.94	.06	.94	.94	.87	.87
	MobileNet	Benign	40	77	8	35	.83	.53	.09	.91	.65	.45	.48
		Malignant	77	40	35	8	.69	.91	.46	.54	.78	.45	.48
		Average Score					.76	.72	.28	.72	.73	.45	.48
	ResNet-50	Benign	47	81	4	28	.92	.63	.05	.95	.75	.59	.62
		Malignant	81	47	28	4	.74	.95	.37	.63	.84	.59	.62
		Average Score					.83	.79	.21	.79	.80	.59	.62
	Xception	Benign	75	80	5	0	.94	1.0	.06	.94	.97	.94	.94
		Malignant	80	75	0	5	1.0	.94	0	1.0	.97	.94	.94
		Average Score					.97	.97	.03	.97	.97	.94	.94
	Proposed method	Benign	74	85	0	1	1.0	.99	0	1.0	.99	.99	.99
		Malignant	85	74	1	0	.99	1.0	.01	.99	.99	.99	.99
		Average Score					.99	.99	.01	.99	.99	.99	.99

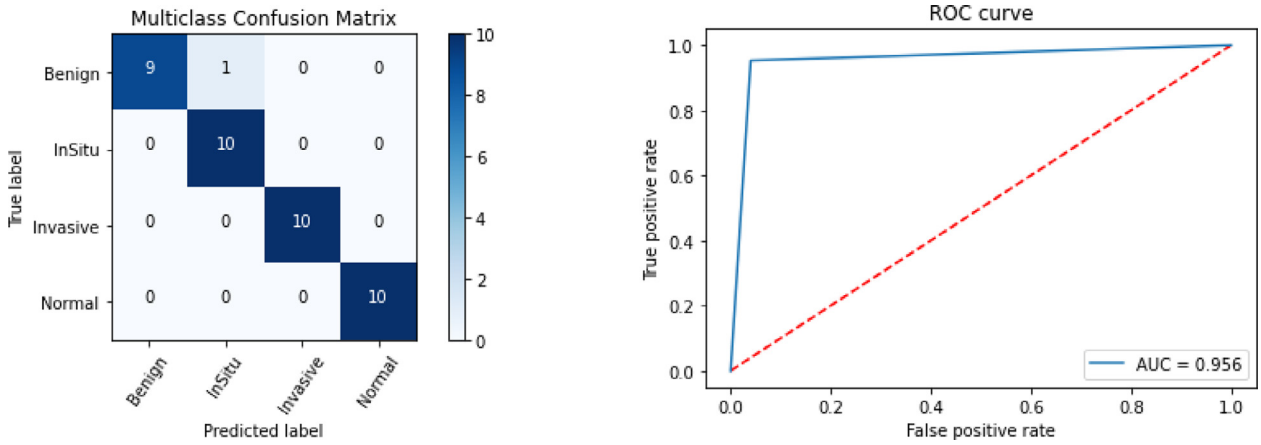

Fig. 7. "MultiNet" performance on ICIAR dataset a) confusion matrix b) ROC curve.

be ineffective when dealing with a large number of images (Dimitropoulos et al., 2017; Karthiga and Narasimhan, 2018; Song et al., 2017; Nahid et al., 2018). The proposed framework provides a segmentation free approach that does not require any handcrafted features. In Mehra (2018), the authors have performed three well-known pre-trained models, including VGG16, VGG19, and ResNet50, in breast cancer histology image classification. Moreover, they have used logistic regression as a classifier, which performed well in binary classification. However, logistic regression may cause trouble while solving the non-linear problem since it has a linear decision surface. Logistic regression also leads to the model being overfitted while dealing with the high dimensional dataset. Although most of the authors have given a considerable effort to train a network, poor results have been obtained after using different architectures (Song et al., 2017; Saxena et al., 2020; Golatkar et al., 2018; Roy et al., 2019; Ferreira et al., 2018). Furthermore, in Saini and Susan (2020), the authors have employed Deep Convolution Generative Adversarial Network (DCGAN) to solve the data imbalance issue in the BreakHis dataset. They have performed DCGAN only for the data augmentation of the minority class. Since only a few samples are available in the minority class, the distribution of DCGAN training would not be able to generalize well and would not yield high-quality sample images (Saini and Susan, 2020). In another research, Alzubaidi et al. have proposed a hybrid CNN model consisting of 74 layers for the multiclass breast cancer classification (Alzubaidi et al., 2020). Such a deep CNN model requires more computational power, which is expensive and time-consuming. All the methods found in the literature have misclassified the malignant breast cancer images, which is more harmful and decrease the survival chances (Dimitropoulos et al., 2017; Karthiga and Narasimhan, 2018; Song et al., 2017; Nahid et al., 2018; Mehra, 2018; Saxena et al., 2020; Golatkar et al., 2018; Roy et al., 2019; Ferreira et al., 2018; Saini and Susan, 2020; Alzubaidi et al., 2020; Yao et al., 2019). However, our proposed framework does not misclassify any malignant images in both BreakHis and ICIAR datasets, respectively. Despite the achievement of the proposed "MultiNet" framework, several drawbacks

Table 7
Results obtained using "MultiNet" architecture and seven individual transfer learning models on ICIAR Dataset.

Metrics	Model	Breast Cancer Category	TP	TN	FP	FN	Precision	Recall	FPR	TNR	F1-Score	Kappa	MCC
ICIAR Dataset	DenseNet-201	Benign	10	28	2	0	.83	1.0	.06	.94	.91	.88	.88
		InSitu	8	30	0	2	1.0	.80	0	1.0	.89	.86	.87
		Invasive	9	28	2	1	.82	.90	.06	.94	.86	.81	.81
		Normal	8	29	1	2	.89	.80	.03	.97	.84	.79	.79
		Average Score					.88	.87	.04	.96	.88	.84	.84
	NasNetMobile	Benign	8	29	1	2	.89	.80	.03	.97	.84	.79	.79
		InSitu	9	21	9	1	.50	.90	.30	.70	.64	.47	.52
		Invasive	4	30	0	6	1.0	.40	0	1.0	.57	.50	.58
		Normal	8	30	1	2	.89	.80	.03	.97	.84	.79	.80
		Average Score					.82	.72	.09	.91	.72	.64	.67
	VGG-16	Benign	7	28	2	3	.78	.70	.07	.93	.74	.66	.66
		InSitu	8	25	5	2	.62	.80	.17	.83	.70	.58	.59
		Invasive	8	25	5	2	.62	.80	.17	.83	.70	.58	.59
		Normal	5	30	0	5	1.0	.50	0	1.0	.67	.60	.65
		Average Score					.75	.70	.10	.90	.70	.61	.62
	VGG-19	Benign	7	25	5	3	.58	.70	.16	.84	.64	.50	.50
		InSitu	4	29	1	6	.80	.40	.03	.97	.53	.44	.48
		Invasive	6	27	3	4	.67	.60	.10	.90	.63	.52	.52
		Normal	9	25	5	1	.64	.90	.16	.84	.75	.65	.67
		Average Score					.67	.65	.45	.55	.65	.53	.54
	MobileNet	Benign	0	29	1	10	0	0	.03	.97	0	-.05	-.09
		InSitu	5	20	10	5	.33	.50	.33	.67	.40	.14	.15
		Invasive	8	17	13	2	.38	.80	.43	.57	.52	.27	.32
		Normal	2	29	1	8	.67	.20	.03	.97	.31	.22	.27
		Average Score					.35	.38	.21	.79	.38	.15	.16
	ResNet-50	Benign	7	28	2	3	.78	.70	.07	.93	.74	.66	.66
		InSitu	8	26	4	2	.67	.80	.13	.87	.73	.63	.63
		Invasive	8	29	1	2	.89	.80	.03	.97	.84	.79	.79
		Normal	9	29	1	1	.90	.90	.03	.97	.90	.87	.87
		Average Score					.84	.80	.07	.93	.80	.74	.74
	Xception	Benign	6	29	1	4	.86	.60	.03	.97	.71	.63	.65
		InSitu	9	25	5	1	.64	.90	.17	.83	.75	.65	.67
		Invasive	9	30	0	1	1.0	.90	0	1.0	.95	.93	.93
		Normal	9	29	1	1	.90	.90	.03	.97	.90	.87	.87
		Average Score					.85	.83	.06	.94	.82	.77	.78
	Proposed method	Benign	9	30	0	1	1.0	.90	0	1.0	.95	.93	.93
		InSitu	10	29	1	0	.91	1.0	.03	.97	.95	.94	.94
		Invasive	10	30	0	0	1.0	1.0	0	1.0	1.0	1	1
		Normal	10	30	0	0	1.0	1.0	0	1.0	1.0	1	1
		Average Score					.98	.98	.01	.99	.98	.97	.97

Table 8
Comparison of the proposed "MultiNet" framework with other methods in binary and multi-class classification.

Number	Method	Best Accuracy for BreakHis Dataset	Best Accuracy for ICIAR Dataset	Classification Type	Classification Method
1	Dimitropoulos et al. (2017) 2017	91.38 %		Binary class	VLAD
2	Karthiga and Narasimhan (2018) 2018	93.3%		Binary class	K-means + DWT
3	Song et al. (2017) 2017	86.67%		Binary class	Fisher Vector + CNN
4	Nahid et al. (2018) 2018	91%		Multiclass	CNN + LSTM + Softmax + SVM
5	Mehra (2018) 2018	92.6%		Binary class	VGG16 + Logistic Regression
6	Saini and Susan (2020) 2020	94.5%		Multiclass	DCGAN + VGG16
7	Saxena et al. (2020) 2020	87.4%		Multiclass	ResNet50 + KWELM
8	Alzubaidi et al. (2020) 2020		96.1%	Multiclass	Hybrid CNN
9	Golatkar et al. (2018) 2018		85%	Multiclass	Inception-V3
10	Roy et al. (2019) 2019		87%	Multiclass	CNN
11	Yao et al. (2019) 2019		97.25%	Multiclass	CNN + RNN + Attention
12	Ferreira et al. (2018) 2018		76%	Multiclass	Inception ResNet V2
13	Proposed Framework	99%		Binary class	DenseNet-201 + NasNetMobile + VGG-16 + Fine-tuned
14	Proposed Framework		98%	Multiclass	DenseNet-201 + NasNetMobile + VGG-16 + Fine-tuned

can be addressed in future studies. For example, the BreakHis dataset has a data imbalance issue that we can overcome by introducing DCGAN for data augmentation on both majority and minority classes. We only use 200 epochs to train the model for the ICIAR dataset. Further training may improve the accuracy of the model.

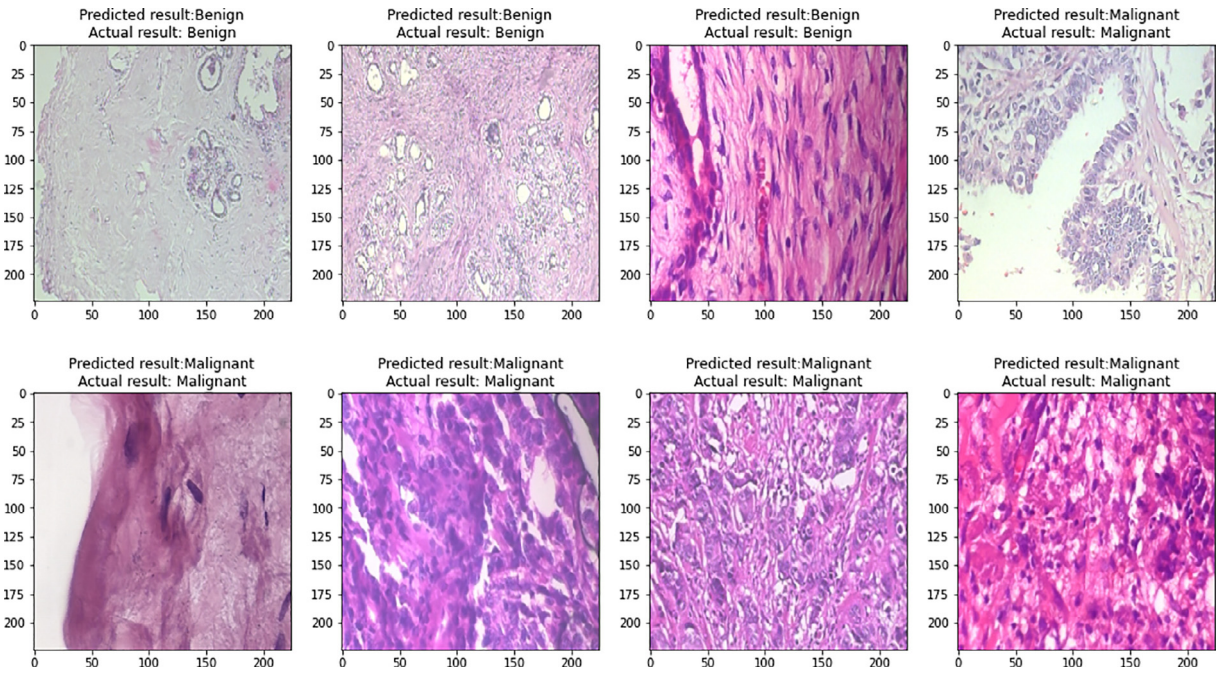

Fig. 8. "MultiNet" evaluated some microscopy images.

6. Conclusion

In this work, we have proposed a novel deep "MultiNet" framework to detect breast cancer cases from microscopy images more precisely and reliably. The proposed "MultiNet" framework is based on a transfer learning and feature extraction technique that allows different pre-trained CNN models to extract features parallelly and finally combined them for the classification task. The model has been trained and tested on both small and large numbers of image datasets. It is designed in such a way that it can operate effectively on diverse datasets. Experimental results demonstrate that the "MultiNet" framework achieves 99% and 98% classification accuracy in the BreakHis and ICIAR datasets, respectively, outperforming both individual CNN pre-trained architectures and all the other stat—of—the—art models found in the literature. Moreover, it exhibits promising performance in identifying malignant images, increasing the survival chance. Based on such encouraging results, we believe that our "MultiNet" model would be an outstanding candidate that can help the doctor to diagnose and detect breast cancer in a short time.

Data availability

We made all the materials publicly accessible for helping the research community at the following GitHub link: https://github.com/saikat15010/MultiNet-Architecture.git.

Declaration of Competing Interest

The authors declare that they have no known competing financial interests or personal relationships that could have appeared to influence the work reported in this paper.

References

Alzubaidi, L., Al-Shamma, O., Fadhel, M.A., Farhan, L., Zhang, J., Duan, Y., 2020. Optimizing the performance of breast cancer classification by employing the same domain transfer learning from hybrid deep convolutional neural network model. Electronics 9 (3), 445.

Arauo, T., Aresta, G., et al., 2017. Classification of breast cancer histology images using convolutional neural networks. PLoS ONE 12 (6), e0177544.

Aytar, Y., Vondrick, C., Torralba, A., 2016. Soundnet: learning sound representations from unlabeled video. Adv. Neural Inf. Process. Syst. 29, 892–900.

Bhargava, R., Madabhushi, A., 2016. Emerging themes in image informatics and molecular analysis for digital pathology. Ann. Rev. Biomed. Eng. 18, 387–412.

Brancati, N., De Pietro, G., Frucci, M., Riccio, D., 2019. A deep learning approach for breast invasive ductal carcinoma detection and lymphoma multi-classification in histological images. IEEE Access 7, 44 709–44 720.

Bray, F., Ferlay, J., Soerjomataram, I., Siegel, R.L., Torre, L.A., Jemal, A., 2018. In: CA: Cancer J. Clin., pp. 394–424.

Breast cancer facts. [Online]. Available: URL: https://www.nationalbreastcancer.org/breast-cancer-facts.

Breast cancer histopathological database (breakhis). [Online]. Available: URL: https://web.inf.ufpr.br/vri/databases/breast-cancer-histopathological-database-breakhis.

Celik, Y., Talo, M., Yildirim, O., Karabatak, M., Acharya, U.R., 2020. Automated invasive ductal carcinoma detection based using deep transfer learning with whole-slide images. Pattern Recogn. Lett.

Chetlen, A., Mack, J., Chan, T., 2016. Breast cancer screening controversies: who, when, why, and how? Clin. Imag. 40 (2), 279–282.

Collaboration, S.I. et al., 2018. Machine learning and health care disparities in dermatology.

Dimitropoulos, K., Barmpoutis, P., Zioga, C., Kamas, A., Patsiaoura, K., Grammalidis, N., 2017. Grading of invasive breast carcinoma through grassmannian vlad encoding. PloS one 12, (9) e0185110.

Ferreira, C.A., Melo, T., Sousa, P., Meyer, M.I., Shakibapour, E., Costa, P., Campilho, A., 2018. Classification of breast cancer histology images through transfer learning using a pre-trained inception resnet v2. In: International Conference Image Analysis and Recognition. Springer. pp. 763–770.

Gao, M., Bagci, U., Lu, L., Wu, A., Buty, M., Shin, H.-C., Roth, H., Papadakis, G.Z., Depeursinge, A., Summers, R.M., et al., 2018. Holistic classification of ct attenuation patterns for interstitial lung diseases via deep convolutional neural networks. Comput. Methods Biomech. Biomed. Eng. 6 (1), 1–6.

Golatkar, A., Anand, D., Sethi, A., 2018. Classification of breast cancer histology using deep learning. In: International Conference Image Analysis and Recognition. Springer. pp. 837–844.

Hao, W., Zhang, Z., 2019. Spatiotemporal distilled dense-connectivity network for video action recognition. Pattern Recogn. 92, 13–24.

Huang, G., Liu, Z., Van Der Maaten, L., Weinberger, K.Q., 2017. Densely connected convolutional networks. In: Proceedings of the IEEE conference on computer vision and pattern recognition, pp. 4700–4708.

Iciar 2018 grand challenge dataset. [Online]. Available: URL: https://iciar2018-challenge.grand-challenge.org/Home/.

Irshad, H., Veillard, A., Roux, L., Racoceanu, D., 2013. Methods for nuclei detection, segmentation, and classification in digital histopathology: a review—current status and future potential. IEEE Rev. Biomed. Eng. 7, 97–114.

Kandel, I., Castelli, M., 2020. A novel architecture to classify histopathology images using convolutional neural networks. Appl. Sci. 10 (8), 2929.

Karthiga, R., Narasimhan, K., 2018. Automated diagnosis of breast cancer using wavelet based entropy features. In: 2018 Second International Conference on

Electronics, Communication and Aerospace Technology (ICECA). IEEE. pp. 274–279.
Karim, R., Shahrior, A., Rahman, M.M., 2021. Machine learning-based tri-stage classification of Alzheimer's progressive neurodegenerative disease using PCA and mRMR administered textural, orientational, and spatial features. International Journal of Imaging Systems and Technology.
Khan, S., Islam, N., Jan, Z., Din, I.U., Rodrigues, J.J.C., 2019. A novel deep learning based framework for the detection and classification of breast cancer using transfer learning. Pattern Recogn. Lett. 125, 1–6.
Khan, M.S.I., Rahman, A., Karim, M.R., Bithi, N.I., Band, S., Dehzangi, A., Alinejad-Rokny, H., 2021. Covidmulti-net: a parallel-dilated multi scale feature fusion architecture for the identification of covid-19 cases from chest x-ray images. medRxiv.
Khan, M.S.I., Islam, N., Uddin, J., Islam, S. and Nasir, M.K., 2021. Water quality prediction and classification based on principal component regression and gradient boosting classifier approach. Journal of King Saud University-Computer and Information Sciences.
Komura, D., Ishikawa, S., 2018. Machine learning methods for histopathological image analysis. Comput. Struct. Biotechnol. J. 16, 34–42.
LeCun, Y., Bengio, Y., Hinton, G., 2015. Deep learning. Nature 521 (7553), 436–444.
Liu, Z., Luo, P., Wang, X., Tang, X., 2015. Deep learning face attributes in the wild. In: Proceedings of the IEEE international conference on computer vision, pp. 3730–3738.
López, C., Lejeune, M., Bosch, R., Korzynska, A., García-Rojo, M., Salvadó, M.-T., Álvaro, T., Callau, C., Roso, A., Jaén, J., 2012. Digital image analysis in breast cancer: an example of an automated methodology and the effects of image compression. Stud. Health Technol. Inf. 179, 155.
Lumini, A., Nanni, L., 2019. Deep learning and transfer learning features for plankton classification. Ecol. Inf. 51, 33–43.
McCann, M.T., Ozolek, J.A., Castro, C.A., Parvin, B., Kovacevic, J., 2014. Automated histology analysis: opportunities for signal processing. IEEE Signal Process. Mag. 32 (1), 78–87.
Mehra, R. et al., 2018. Breast cancer histology images classification: training from scratch or transfer learning? ICT Express 4 (4), 247–254.
Motlagh, M.H., Jannesari, M., Aboulkheyr, H., Khosravi, P., Elemento, O., Totonchi, M., Hajirasouliha, I., 2018. Breast cancer histopathological image classification: a deep learning approach. BioRxiv, 242818.
Nahid, A.-A., Mehrabi, M.A., Kong, Y., 2018. Histopathological breast cancer image classification by deep neural network techniques guided by local clustering. BioMed Res. Int. 2018.
Pereira, S., Pinto, A., Alves, V., Silva, C.A., 2016. Brain tumor segmentation using convolutional neural networks in mri images. IEEE Trans. Med. Imag. 35 (5), 1240–1251.
Pöllänen, I., Braithwaite, B., Ikonen, T., Niska, H., Haataja, K., Toivanen, P., Tolonen, T., 2014 Computer-aided breast cancer histopathological diagnosis: Comparative analysis of three dtocs-based features: Sw-dtocs, sw-wdtocs and sw-3-4-dtocs. In: 2014 4th International Conference on Image Processing Theory, Tools and Applications (IPTA). IEEE. pp. 1–6.
Robbins, P., Pinder, S., De Klerk, N., Dawkins, H., Harvey, J., Sterrett, G., Ellis, I., Elston, C., 1995. Histological grading of breast carcinomas: a study of interobserver agreement. Human Pathol. 26 (8), 873–879.
Roy, K., Banik, D., Bhattacharjee, D., Nasipuri, M., 2019. Patch-based system for classification of breast histology images using deep learning. Comput. Med. Imaging Graph. 71, 90–103.
Saini, M., Susan, S., 2020. Deep transfer with minority data augmentation for imbalanced breast cancer dataset. Appl. Soft Comput. 97, 106759.
Saxena, S., Shukla, S., Gyanchandani, M., 2020. Breast cancer histopathology image classification using kernelized weighted extreme learning machine. Int. J. Imaging Syst. Technol.
Saxen, F., Werner, P., Handrich, S., Othman, E., Dinges, L., Al-Hamadi, A., 2019. Face attribute detection with mobilenetv2 and nasnet-mobile. 11th International Symposium on Image and Signal Processing and Analysis (ISPA), IEEE 2019, 176–180.
Scherer, D., Müller, A., Behnke, S., 2010. Evaluation of pooling operations in convolutional architectures for object recognition. In: International conference on artificial neural networks. Springer. pp. 92–101.
Siegel, R., Naishadham, D., Jemal, A., 2012. Ca cancer. Cancer Stat.
Simonyan, K., Zisserman, A., 2014. Very deep convolutional networks for large-scale image recognition. arXiv preprint arXiv:1409.1556.
Song, Y., Zou, J.J., Chang, H., Cai, W., 2017. Adapting fisher vectors for histopathology image classification. IEEE 14th International Symposium on Biomedical Imaging (ISBI 2017), IEEE 2017, 600–603.
Srivastava, N., Hinton, G., Krizhevsky, A., Sutskever, I., Salakhutdinov, R., 2014. Dropout: a simple way to prevent neural networks from overfitting. The journal of machine learning research 15 (1), 1929–1958.
Szczypiński, P., Klepaczko, A., Pazurek, M., Daniel, P., 2014. Texture and color based image segmentation and pathology detection in capsule endoscopy videos. Comput. Methods Programs Biomed. 113 (1), 396–411.
Talo, M., 2019. Automated classification of histopathology images using transfer learning. Artif. Intell. Med. 101, 101743.
Veta, M., Pluim, J.P., Van Diest, P.J., Viergever, M.A., 2014. Breast cancer histopathology image analysis: a review. IEEE Trans. Biomed. Eng. 61 (5), 1400–1411.
Wang, Z., Dong, N., Dai, W., Rosario, S.D., Xing, E.P., 2018. Classification of breast cancer histopathological images using convolutional neural networks with hierarchical loss and global pooling. In: International Conference Image Analysis and Recognition. Springer. pp. 745–753.
W.H. Organization et al., 2014. WHO position paper on mammography screening. World Health Organization.
Wong, S.C., Gatt, A., Stamatescu, V., McDonnell, M.D., 2016. Understanding data augmentation for classification: when to warp? 2016 international conference on digital image computing: techniques and applications (DICTA), IEEE 2016, 1–6.
Yao, H., Zhang, X., Zhou, X., Liu, S., 2019. Parallel structure deep neural network using cnn and rnn with an attention mechanism for breast cancer histology image classification. Cancers 11 (12), 1901.
Yildirim, O., Baloglu, U.B., Tan, R.-S., Ciaccio, E.J., Acharya, U.R., 2019. A new approach for arrhythmia classification using deep coded features and lstm networks. Comput. Methods Programs Biomed. 176, 121–133.
Zoph, B., Vasudevan, V., Shlens, J., Le, Q.V., 2018. Learning transferable architectures for scalable image recognition. In: Proceedings of the IEEE conference on computer vision and pattern recognition, pp. 8697–8710.